7 Search for the rare decay $\mu^+ \to e^+e^-e^+$

R. Gredig, P. Robmann, and U. Straumann

in collaboration with: University of Geneva, Paul Scherrer Institute, ETH Zürich, University of Heidelberg, University of Mainz, Karlsruhe Institute of Technology

(Mu3e Collaboration)

Mu3e is a proposed experiment searching for the charged-lepton-flavour violating decay $\mu^+ \to e^+e^-e^+$, aiming at a sensitivity to its branching ratio B down to 10^{-16} and better [1]. In the standard model charged lepton flavour violation is highly suppressed, so a discovery would clearly present physics beyond the standard model. The aimed sensitivity is four orders of magnitude beyond the limit set by the SINDRUM experiment [2]. Muon number violation has already been searched in many channels and recently MEG, for example, set an upper limit of 5.7×10^{-13} in the $\mu^+ \to e^+\gamma$ channel [3].

7.1 Scintillating Fibres

The University of Zurich is mainly involved in developing a scintillating fibre detector located in the center module of the detection setup (see Fig. 7.1). The fibres will be combined to 16 mm wide ribbons, containing three or four layers. Currently, different types of fibres are under investigation. Whereas the universities of Geneva and Zurich and ETHZ focus on round 250 µm thick doubly cladded fibres, with the option of an additional titanium dioxide coating, the Paul Scherrer Institute (PSI) investigates square fibres.

7.2 Fibre Ribbon Performance Testing

In the past year a test setup has been developed for the examination of several multi-layer fibre ribbons matching the final design (three to four layers, 16 mm wide). 32 fibres can be read out on both ends. The photons are detected with a modular three stage system. The first stage is a board holding the silicon photomultipliers (SiPMs) and a high voltage distribution system. The second stage is a PCB directly connected to this sensor-board, containing a signal amplifier that can drive a 50 Ω signal cable. The third stage digitizes the data with eight daisy chained DRS4 evaluation boards [4] and an additional DRS4 board recording the trigger signals.

The ribbon performance has been tested by irradiation with a ^{90}Sr-source and at the PSI piM1 test-area with a beam momentum of 161 MeV/c. The goal was to measure the light yield and time resolution and check the simulation results presented in last years Annual Report.

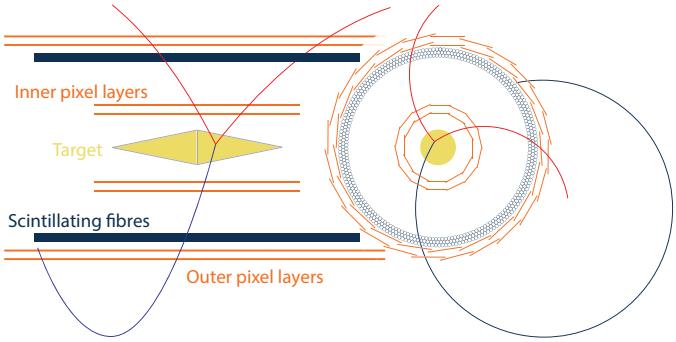

FIG. 7.1 – Central region of the Mu3e setup in the zy and xy projections. The central fibre tracker consists of three layers of 250 µm fibres with a length of 36 cm.

7.2.1 Readout electronics

The second generation sensor-board, shown in Fig.7.2 holds 16 individual SiPMs (the first generation board had a monolithic 4x4 SiPM module) that can be biased individually. The small sensitive area of only $1 \times 1\,\text{mm}^2$ results in a relatively low dark-count rate of $\mathcal{O}(10^5)$ photoelectrons. A third version of the board will allow to connect a variety of DAQ systems including different ASICs considered for the final design.

Because of the lack of a common clock on all boards, it was unclear how precisely the trigger signal propagates through them, so this had to be measured. A test-pulse was split in two and the resolution of the time difference Δt was found to be $\sigma_{\Delta t} \approx 232$ ps. Assuming that all channels have a resolution σ_t, the resolution of the DAQ system is $\sigma_t = \sigma_{\Delta t}/\sqrt{2} \approx 165$ ps.

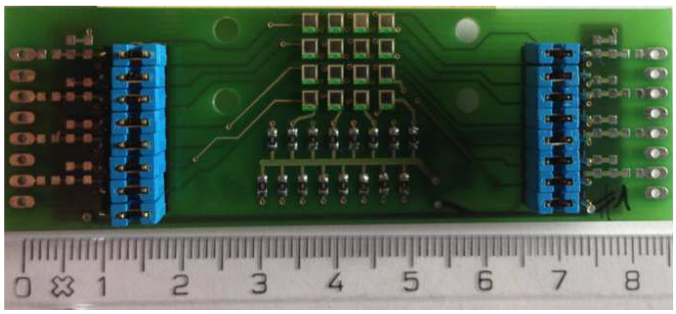

FIG. 7.2 – Second generation sensor-board with 16 individual $1 \times 1\,\text{mm}^2$ sensors.

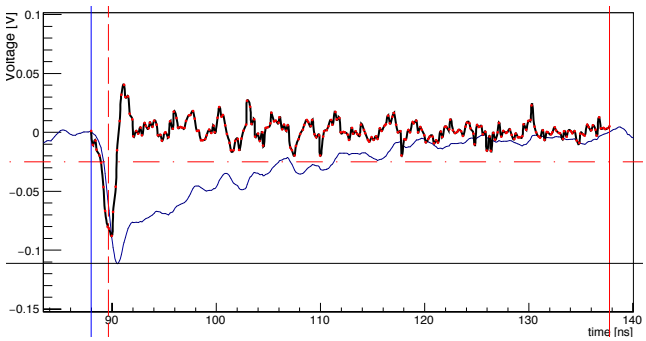

FIG. 7.3 – A fibre waveform. Both the original (blue) and the differentiated signal (black) are shown. Various observables are determined. The signal amplitude (horizontal black line) is the minimal value of the original waveform. The signal time (vertical dashed red line) is the centroid of the negative peak in the differentiated waveform. The signal integral is the sum of the original waveform over the window marked by the vertical blue and red lines.

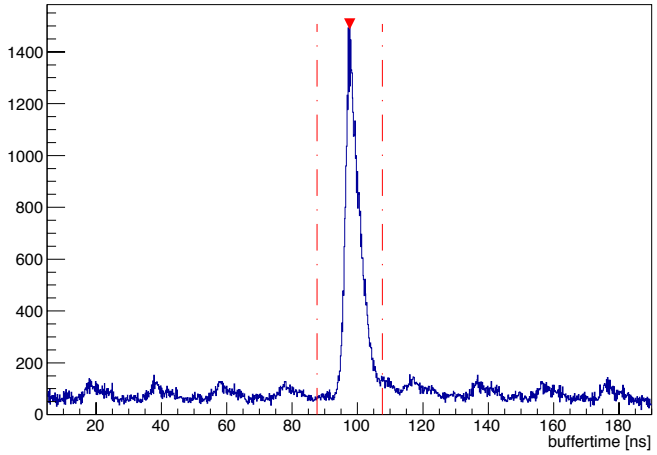

FIG. 7.4 – Time difference between fibre signals crossing a threshold just above the electric noise and a reference trigger counter. The periodic structure of accidental coincidences results from the 50 MHz PSI cyclotron frequency. The red markers show the window used in this analysis.

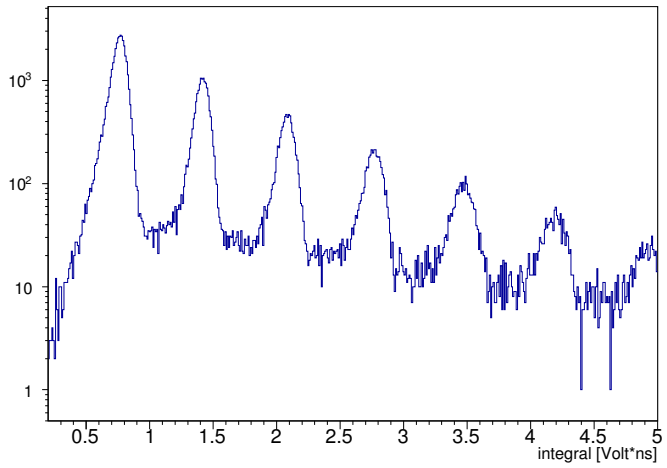

FIG. 7.5 – Histogram of signal integrals for one of the fibres showing well-separated peaks associated with the number of observed photo-electrons.

7.2.2 Signal Analysis

Figure 7.3 shows a typical waveform produced with the PSI positron beam. Under investigation was Kurary SCSF-81 Multi Clad. In most events the positron triggering a small downstream beam counter did not cross the fibre under study so off-line a -25 mV threshold was set on the amplitude (red dash-dotted line in Fig.7.3) to remove events with noise only. The distribution of the times when the signal crossed that threshold for the first time (Fig.7.4) shows a pronounced prompt peak on a random background. For further analysis events are selected from the prompt window indicated in Fig.7.4. The distribution of the signal integral (Fig. 7.5) shows a series of peaks associated with the number of detected photo-electrons. These distributions allow an accurate gain calibration for each fibre. In further discussions the number of photo-electrons is used as a measure of the signal amplitude.

7.3 Results

7.3.1 Photon Yield

The observed distribution of the number of photo-electrons is compared with the results of a simulation in Fig.7.6. The current simulation significantly overestimates the signal. It accounts for the SiPM window index of refraction and assumes a photon detection efficiency of 35 %. We have checked that the observed light attenuation over a distance of 355 mm is reproduced by the simulation and suspect that the mismatch is due either to an overestimation of the scintillation yield or an underestimation of light trapping at the beginning.

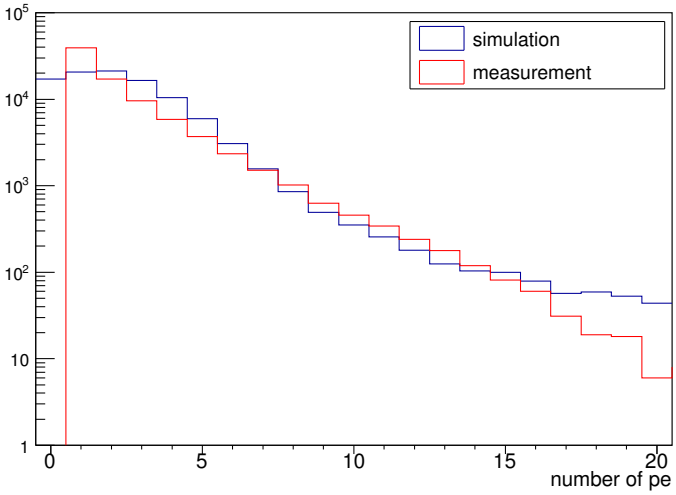

FIG. 7.6 – Measured and predicted distributions of the number of photo-electrons at one fibre end for central ribbon crossing. In the measurement the number of entries with no signal can not be determined from these measurements. The comparison indicates an unknown loss by a factor 3.

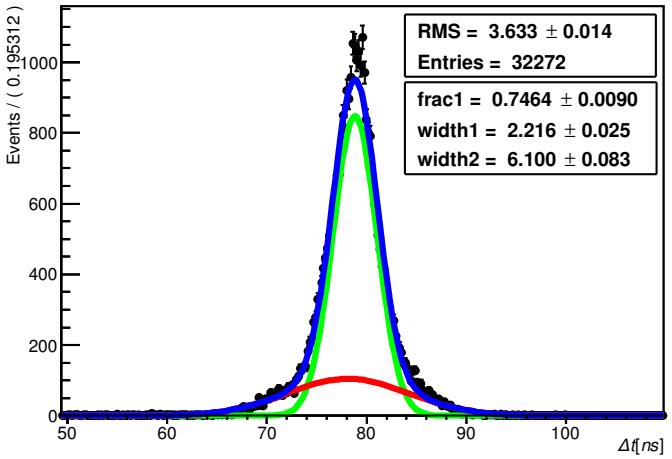

FIG. 7.7 – Distribution of the time difference between the signals from both ends for central ribbon crossing. The observed distribution has been described by two Gaussians with σ=**width**.

7.3.2 Time resolution

The time resolution for a single fibre, given by the observed resolution of the time difference between the signals at both ends of a fibre (Fig.7.7) divided by two, is still above the design goal of 1 ns for a single fibre. An ongoing measurement of the time resolution of SiPM and amplifier alone will help to identify the main contribution to the time resolution.

7.3.3 2015 PSI Test Beam Campaign

For 2015 another test beam campaign at PSI is planned with new ribbons coated with titanium dioxide that will increase the photon yield. In this beam period one of the ASIC candidates, the STiC chip [5], will be tested as well.

[1] A. Blondel *et al.* (Mu3e Collaboration), *Research Proposal for an Experiment to Search for the Decay $\mu \to 3e$*, submitted to PSI (2013), ArXiv 1301.6113.

[2] U. Bellgardt *et al.* (SINDRUM Collaboration), Nucl. Phys. B299 (1988) 1.

[3] J. Adam *et al.* (MEG Collaboration), Phys. Rev. Lett. 110, 201801.

[4] S. Ritt *et al.*, Nucl. Instrum. Methods A 623 486488.

[5] T. Harion *et al.*, 2014 JINST 9 C02003.